A survey of commercial soda–lime–silica glass compositions: Trends and opportunities II—Principal component analysis (PCA) of glass compositions

DENG, Wei, WAKELIN, Elliot, KILINC, Erhan and BINGHAM, Paul A. <http://orcid.org/0000-0001-6017-0798>

Received: 13 June 2024 | Revised: 7 August 2024 | Accepted: 4 September 2024

DOI: 10.1111/ijag.16689

INTERNATIONAL JOURNAL OF Applied Glass SCIENCE

RESEARCH ARTICLE

A survey of commercial soda–lime–silica glass compositions: Trends and opportunities II—Principal component analysis (PCA) of glass compositions

Wei Deng | **Elliot Wakelin** | **Erhan Kilinc** | **Paul A. Bingham**

Materials and Engineering Research Institute, Sheffield Hallam University, Sheffield, UK

Correspondence
Wei Deng and Paul A. Bingham, Materials and Engineering Research Institute, Sheffield Hallam University, Sheffield, S1 1WB, UK.
Email: wei.deng@shu.ac.uk and p.a.bingham@shu.ac.uk

Funding information
UKRI/EPSRC, Grant/Award Number: EP/V054627/1

Abstract

In the first part of the study, we sampled and investigated the composition of commercial glasses in the UK market from 2022 to 2023, as well as property data provided by various models. In this part, we utilize principal component analysis (PCA) to conduct a comparative analysis, integrating these data with the composition of commercial glass documented in previous literature. The widely held belief that the composition of commercial soda–lime–silica glasses has remained essentially unchanged over the past 30+ years is challenged by this research. The differences in composition of current commercial glass compositions compared to glasses from 30 to 40 years ago have been quantified. This not only sheds light on the direction of travel and reasons for adjustments to UK glass compositions over recent decades, but it also provides insights and predictions into the future trends.

KEYWORDS

commercial soda–lime–silica glass, historical industrial glass composition, industrial glass development

1 | INTRODUCTION

For actual compositions of industrial soda–lime–silica glass produced over different periods during the past century, especially container glass, has been notably lacking in publicly available literature during certain periods and particularly over the past three decades. However, if we trace back to earlier literature, an early publicly available survey on the composition of modern industrial glasses goes back to 1920, in which Keppeler[1,2] and Keppeler et al.[3,4] recorded container glass compositions from 1920 to 1941, mainly in Europe. The compositions of US container glasses from 1932 to 1978 were monitored and reviewed by Hartford Empire Co. and Emhart Industries.[5–10] Some of the most important surveys include those by Moore and Lyle who reviewed the period from 1932 to 1946[5]; Allen and Lyle who reviewed 1947,[6] which is particularly interesting due to the shortage of soda ash in 1947; Loesell and Lester who reviewed the period from 1932 to 1960[7]; Lyle[8] who summarized the procedure for the design and development of glasses for manufacture of containers in 1967; and finally, Stadler and Cronin who reviewed glass compositions before 1977.[9,10] During the 1970s to 1980s, Emhart Industries went through a turbulent period, as its revenue in the United States was impacted by the increasing popularity of Polyethylene terephthalate (PET)

containers.[11] As a result, its headquarters were relocated to Zurich, and its survey on American container glass compositions could not be sustained.[11] After that, Katkova et al.[12] introduced former USSR industrial packaging glass compositions and basic trends in 1985. Further publications could not be identified until 2005, when Smrček published his research on European container glasses from 1982 to 1988.[13] Smrček[14–16] also published three comprehensive reviews on the composition of flat, container, and pressed glasses up to 1990 in 2005, and those reviews are some of the most recent surveys in the public domain.

The records and data in the above literature are vital and the sample size in each survey is quite substantial. But the issues present in these studies are also quite significant. Due to commercial confidentialities, individual glass data are not presented in any of those surveys. Compositions are all presented as averages according to time and region, only ranges of components and chemical/physical properties are presented without assignment, which, of course, will have minimized the exposure of information perceived as being commercially sensitive, but a significant amount of corresponding information, especially the compositional differences between glass manufacturers within the same period, same region, and with uniform equipment levels, is not published. This conservatism unfortunately restricts the use of statistical methods for data analysis, further limiting the extraction of available information. For all those surveys, the statistical methods are simple, with the mean and histogram being the most common methods. In a sense, these limitations significantly impact the value of those surveys. Somewhat ironically, any potential perceived perceptions of commercial sensitivity around glass compositions, if they were indeed a contributing factor, have helped drive our present study. Any manufacturer who wishes, or wished, to know the composition of its competitors' products could have simply followed the same approach as we have used in the present study: obtained glass containers and flat glass samples and analyzed them.

Since around 1970, the primary driving force behind changes in the composition of industrial glass raw materials has been cost reduction.[8,17] It has been widely believed that the composition of commercial soda–lime–silica glass has not changed significantly since then. As a result, the perception of commercial soda–lime–silica glass composition has gradually shifted from being dynamic to static. In this work, based on the chemical composition and performance characterization results of current commercial glass samples collected from the UK market between 2022 and 2023 in the first part, principal component analysis (PCA) was used for analysis. Contrary to perceptions within the glass industry and more widely, this study has not only identified differences in the compositions of current commercial glasses, but also found that the range of compositions in current commercial glasses differs from those 30 to 40 years ago. Quantitative analyses have been conducted on the trends in glass compositional changes and their impact on glass properties. The possible reasons for these changes in glass compositions have been further clarified. Moreover, the facts show that glass compositions remain dynamic.

2 | METHODOLOGY

It is well known that mathematics serves as a crucial tool in guiding the advancement of materials science. The essence of the complex glass composition is a set of high-dimensional data according to the percentage of components, directly analyzing and discussing the characteristics of glass compositions based on the high-dimensional glass composition data may unavoidably carry a sense of subjectivity and insufficiently comprehensive; and the challenges precisely lie in this aspect. PCA is a mathematical technique employed for dimensionality reduction or restructuring information in datasets. This analytical method has already started being employed in glass science research.[18–20] PCA serves as a dual-purpose technique, bridging statistics and machine learning. Statistically, PCA transforms data into orthogonal principal components (PCs) that capture the most significant portion of data variability, ordered by variance, offering an avenue to explain data variability. The computation of PCs follows simple guidelines. The first PC represents the direction in the data that explains the highest variability.

The subsequent PCs are orthogonal to the preceding PC and account for the maximum remaining variability.[21] In machine learning, PCA acts as a dimensionality reduction tool for high-dimensional datasets, curbing redundancy, enhancing model performance, and avoiding dimensionality issues. This technique is categorized as unsupervised learning due to its label-independent nature.

In this study, we employ PCA to conduct dimensionality reduction and classification of glass composition. First, we consider each component present in the collected glass samples as a dimension and standardize the data to have zero mean and unit variance. This standardization is crucial as it ensures that all components contribute equally to the analysis, preventing components with larger scales from dominating the PCA results. We then calculate the correlation matrix of the standardized data, which represent the linear relationship between glass components. Through the analysis of the correlation matrix, we can identify the PCs that explain the most variance in the original data, thereby achieving dimensionality reduction and extracting important features related to glass components.

TABLE 1 The historical flint glass composition data for principal component analysis (PCA) in this work are excerpted from tab. 1 in the research by Smrček[15] (in wt%).

Label	SiO_2	Al_2O_3	Fe_2O_3	CaO	MgO	Na_2O	K_2O	SO_3	Sum
68–71GE	68.814	.965	.063	8.761	1.021	18.490	1.886	.000	100
91–99GE	70.384	1.015	.000	8.647	.000	16.888	3.066	.000	100
0915GE	74.188	1.099	.038	8.305	.511	15.235	.624	.000	100
2326GE	73.166	.876	.079	8.969	.479	15.461	.532	.437	100
2731GE	72.873	.663	.056	10.307	.980	13.970	.889	.262	100
3337GE	75.136	.685	.038	9.182	.256	12.756	1.947	.000	100
4650GE	71.824	.832	.060	8.969	.548	16.606	.691	.470	100
7177GE	73.208	.954	.016	11.173	1.604	12.537	.289	.219	100
8082GE	71.947	.913	.022	10.800	2.636	13.143	.344	.195	100
8387GE	72.354	.954	.020	10.570	2.966	12.578	.408	.150	100
8891GE	71.759	1.124	.019	10.666	3.766	12.071	.490	.105	100

Note: "GE" means Germany; "8387GE" means German glass from 1983 to 1987, for 19 century's glasses marked with "–," such as German glass from 1891 to 1899 was labeled as 91–99GE.

PCA scores signify sample positions on PCs, while loadings depict feature importance.

The PCA 95% confidence ellipse visually captures variability and uncertainty, facilitating comprehension of data distribution, patterns, and relationships, thereby enhancing data analysis and decision-making prowess. In addition to clarifying the differences between the current glass compositions that characterized in this work, the average compositions of historical commercial glasses of different regions and time periods from review of Smrček[13–17] were also referenced here. These historical commercial average compositions were included in the PCA analysis alongside the glass compositions of this study. The PCA analysis can be implemented using various software. In our study, we utilized the PCA component of Origin® to achieve data analysis and visualization.

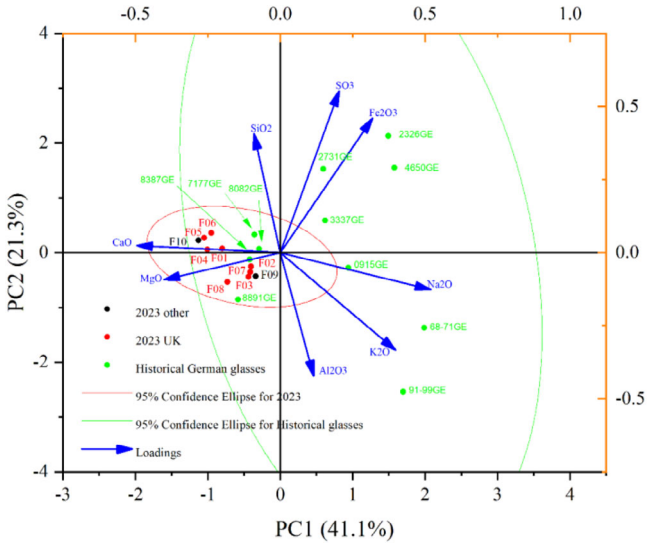

FIGURE 1 Principal component analysis (PCA; PC1 and PC2) biplot of current flint container glasses composition (in red and black) and historical flint glass composition from the record of Smrček[15] (in cyan, and marked according to the year and region, "GE" means Germany; "8387GE" means German glass from 1983 to 1987, for 19 century's glasses marked with "–," such as German glass from 1891 to 1899 was labeled as 91–99GE).

3 | DATA PREPARATION—HISTORICAL COMMERCIAL GLASS COMPOSITION DATA

The historical glass composition data for PCA plots, which excerpted from the comprehensive review work of Smrček,[15] are listed here (all compositions are normalized to 100%) (Tables 1–4).

4 | RESULTS AND DISCUSSION

4.1 | Flint container glasses

As an important part of container glass, flint container glass comprises 64% of total container glass production.[22] Figure 1 presents the PCA analysis results of the compositions of flint container glasses. PC1 and PC2 refer to the first and second PCs, respectively. PC1 represents the direction in the data that capture the most variance, while PC2 represents the direction orthogonal (perpendicular) to PC1 that captures the second most variance, and so on. Historical glass composition data of flint glasses from Smrček's review[15] are included in the diagram for reference and comparison purposes.

The current flint glass compositions are predominantly clustered along the negative axis of the horizontal

TABLE 2 The historical green glass composition data for principal component analysis (PCA) in this work are excerpted from tab. 5 in the research by Smrček[15] (in wt%).

Label	SiO_2	Al_2O_3	Fe_2O_3	CaO	MgO	Na_2O	K_2O	SO_3	Sum
84–89GE	58.580	8.200	2.050	17.300	1.530	10.090	2.250	.000	100
89–91GE	63.130	3.410	3.020	15.400	2.240	9.630	3.170	.000	100
0409GE	64.160	7.370	2.190	14.640	2.140	7.930	1.570	.000	100
1013GE	62.390	8.820	1.670	15.040	2.150	7.630	2.300	.000	100
15GE	63.590	9.350	1.870	13.930	2.700	7.620	.950	.000	100
2425GE	63.830	7.320	1.580	14.840	1.240	9.500	1.190	.510	100
2627GE	64.590	6.180	2.020	12.840	1.500	10.230	2.130	.510	100
2829GE	65.160	6.110	2.050	12.700	.980	10.630	2.370	.000	100
3032GE	63.750	7.340	2.120	13.710	1.330	8.860	2.390	.500	100
3437GE	64.360	6.960	2.270	15.790	.710	8.170	1.740	.000	100
4550GE	65.630	5.900	1.050	11.780	.900	12.630	1.720	.390	100
7077GE	72.100	2.150	.370	10.250	1.620	12.560	.740	.210	100
8290GE	71.680	2.320	.350	9.900	2.290	12.500	.860	.100	100
8387IT	69.601	2.988	.361	9.364	2.567	13.806	1.203	.110	100
88UK	72.142	1.852	.310	10.561	1.121	13.383	.601	.030	100
7190CZ	71.479	2.056	.491	8.795	2.708	13.558	.662	.251	100

Note: "G" means Germany; "It" means Italy; "CZ" means Czechia; "1013G" means German glass from 1910 to 1913, for 19 century's glasses marked with "–," such as German glass from 1889 to 1891 was labeled as 89–91G.

TABLE 3 The historical amber glass composition data for principal component analysis (PCA) in this work are excerpted from tab. 4 in the research by Smrček[15] (in wt%).

Label	SiO_2	Al_2O_3	Fe_2O_3	CaO	MgO	Na_2O	K_2O	SO_3	Sum
13GE	70.166	3.373	.000	8.581	1.327	16.554	.000	.000	100
2537GE	72.974	.680	.200	6.987	1.509	16.752	.900	.000	100
4650GE	72.411	1.623	.242	7.835	.222	16.628	1.039	.000	100
7283GE	72.322	1.854	.271	10.302	1.423	13.198	.581	.050	100
8490GE	71.320	2.268	.331	10.406	2.308	12.484	.863	.020	100
2630UK	71.828	1.803	.371	9.935	.691	15.373	.000	.000	100
8088UK	72.766	1.881	.250	10.965	.190	12.846	1.061	.040	100
6889IT	71.351	1.500	.079	10.056	3.030	13.244	.725	.015	100
7888FR	72.371	1.987	.151	11.050	1.094	12.906	.391	.050	100
7189CZ	72.975	1.423	.231	7.348	3.949	13.543	.491	.040	100
88BE	72.046	1.770	.201	8.497	2.504	14.550	.422	.010	100
83DK	71.513	2.370	.229	10.306	2.250	12.536	.797	.000	100

Note: Marked according to the year and region, "GE" means Germany, "IT" means Italy, "BE" means Belgium, "CZ" means Czechia, "DK" means Denmark, and "FR" means France.

coordinate, while most historical glass compositions are situated in quadrants 1 and 4. Moreover, when compared to other historical glass compositions, the current glass compositions form clusters that align with those from 1971 to 1991. By focusing on this region, as depicted in Figure 2, the current glass compositions segregate into two distinct clusters. Cluster 1 comprises F03, F07, F02, and F09, which are closely associated with the glass compositions from 1971 to 1991. The second cluster includes F10, F05, F04, F06, and F01, and it is separated from Cluster 1. F08 stands alone as an isolated composition.

These findings suggest that a portion of the current flint glass compositions (Cluster 2) already differ from the flint glass compositions of 1977–1991. However, another portion of the current glass compositions (Cluster 1) falls within the range of the previous compositions, indicating that the compositions in Cluster 1 are similar to those from 1977 to 1991 compared to Cluster 2. Cluster 2 represents current

TABLE 4 The historical float glass composition data for principal component analysis (PCA) in this work are excerpted from tab. 6 in the research by Smrček[14] (in wt%).

Label	SiO_2	Al_2O_3	Fe_2O_3	CaO	MgO	Na_2O	K_2O	SO_3	Sum
8687GE	72.324	.460	.080	8.552	4.451	13.753	.120	.260	100
8799GE	72.650	.561	.102	8.772	3.975	13.559	.220	.160	100
7683FR	71.259	.370	.081	9.620	4.080	14.100	.120	.370	100
6099UK	72.532	1.189	.128	8.661	3.596	13.036	.619	.240	100
8387BE	71.406	.651	.066	9.499	4.018	13.888	.210	.261	100
8399IT	71.730	1.094	.104	8.924	3.955	13.431	.522	.241	100
84US	72.931	.190	.122	8.572	4.066	13.639	.000	.481	100
87NL	71.107	.863	.062	8.690	4.987	13.949	.100	.241	100
89CH	72.894	1.162	.102	8.377	3.868	12.996	.401	.200	100
71–90CZ	72.637	.760	.049	8.454	3.882	13.657	.320	.240	100

Note: Marked according to the year and region, "GE" means Germany, "FR" means France, "BE" means Belgium, "IT" means Italy, "CZ" means Czechia, "CH" means Switzerland, and "NL" means the Netherlands.

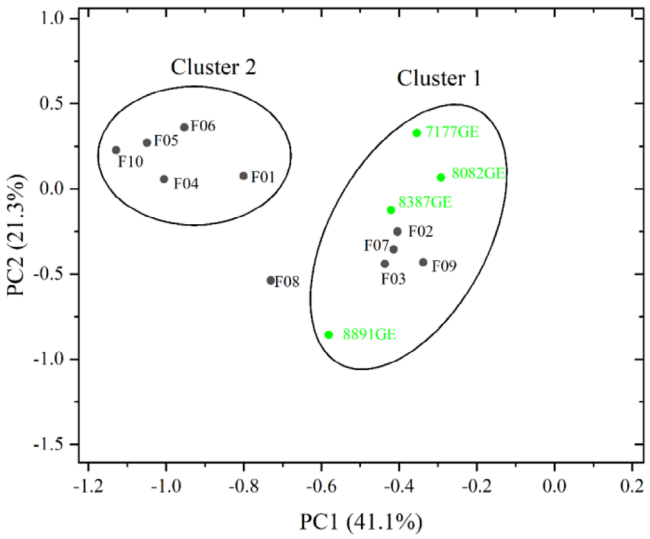

FIGURE 2 Zoom in principal component analysis (PCA) score plot of current flint container glasses composition (in black) and historical flint glass composition from the record of Smrček since 1971.[15] (The strategy of amplifying rather than redoing PCA considers and preserves the influence of historical glass data in the overall composition distribution of existing glasses.)

trends in the development of flint glass compositions for container glass production.

To enhance the understanding of trends and variations in the evolution of constituents, the results obtained by unfolding the glass compositions of this study in the direction of the first PC (PC1), from small to large, are presented in Table 5. The sequential variations in glass compositions clearly demonstrate a discernible pattern. Specifically, Cluster 2 shows an average Al_2O_3 wt% of 1.253 wt%, which is notably lower than the 1.671 wt% observed in Cluster 1. Furthermore, Cluster 2 has an average Na_2O wt% of 12.274 wt%, which is lower than the 13.332 wt% in Cluster 1. Cluster 2 exhibits an average MgO wt% of 1.787 wt%, which is notably higher than the 1.238 wt% in Cluster 1. For CaO, Cluster 2 displays an average of 11.489 wt%, which is slightly higher than the 11.012 wt% in Cluster 1.

It is important to note that the primary distinction between the two clusters is evident in PC1, and the contribution of each component vector to PC1 is consistent with the analysis results mentioned above. In summary, the trends observed in the evolution of flint container glass constituents, as revealed by PCA, relative to the historical composition from 1971 to 1991 and some of the current glass compositions (Cluster 1), can be summarized as follows: decreased aluminum content, comparatively lower sodium content, reduced magnesium content, and slightly elevated calcium content.

Concerning regional differences, first, the Indian glass that falls into Cluster 1 is an anomalous data point compared to the others. Although its compositional characteristics are closer to Cluster 1 compared to Cluster 2, it undoubtedly "deviates further." It exhibits significantly lower Al_2O_3 and the lowest CaO among other Cluster 1 glasses. Among all the glasses, F09 has the lowest SiO_2, highest MgO, and Na_2O content. If we extend our observations of glass composition to PC3 as shown in Figure 3. The proportion of PC3, which accounts for 15.6% of the variance in the interpretation system, indicates that the composition of Indian samples in the PC3 direction is different from Cluster 1, 2, and even most historical compositions. It occupies a unique domain in the PC space of 1, 2, and 3, which collectively explain 78% of the variance in the interpretation system.

Directly observing F09 without utilizing PCA would lead to it being perceived as significantly deviating from the average value of other glass compositions, making its classification into any specific glass category impossible. However, by employing PCA technique, not only was F09

TABLE 5 Flint container glass compositions of this study in the direction of principal component 1 (PC1).

Region	Denmark	United Kingdom	United Kingdom	United Kingdom	United Kingdom	United Kingdom	United Kingdom	United Kingdom	United Kingdom	India
	Cluster 2						Cluster 1			
Sample (wt%)	F10	F05	F04	F06	F01	F08	F02	F07	F03	F09
SiO_2	72.707	72.654	72.597	72.738	71.945	72.459	72.693	72.552	71.977	70.378
Al_2O_3	1.215	1.241	1.372	1.209	1.229	1.533	1.6(	1.725	1.741	1.531
Fe_2O_3	.057	.067	.059	.077	.07	.027	.058	.057	.068	.129
CaO	11.767	11.715	11.609	11.258	11.095	9.901	11.0	11.153	11.571	10.244
MgO	1.695	1.708	1.688	1.876	1.968	2.258	.676	.71	.762	2.802
Na_2O	11.961	12.026	12.055	12.224	13.106	13.524	13.0(	13.052	13.118	14.071
K_2O	.346	.398	.404	.391	.383	.04	.522	.561	.575	.523
TiO_2	.03(	.05	.059	.049	.057	.044	.0	.053	.055	.072
ZrO_2	.008	.005	.004	.004	.004	.003	.004	.004	.004	.01
SO_3	.20(	.133	.151	.172	.141	.21	.1	.132	.126	.239
Cr_2O_3	.002	.003	.002	.002	.002	.001	.002	.001	.003	.001
Sum	100	100	100	100	100	100	100	100	100	100

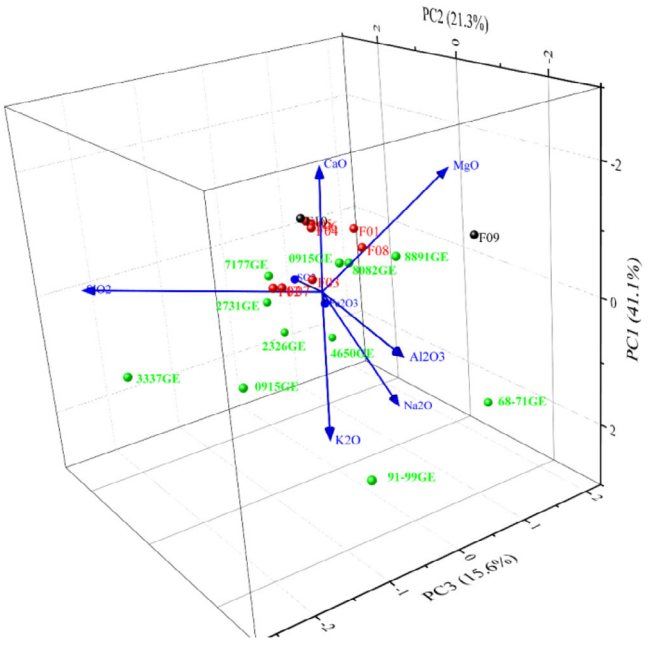

FIGURE 3 Principal component analysis (PCA; PC1, PC2, and PC3) of current flint container glasses composition (in red and black) and historical flint glass composition from the record of Smrček.[15]

successfully clustered, but it also unveiled its homogeneity with glass compositions from 1971 to 1991 years and certain current UK glasses in 2D PCA diagram, which explained 62.4% of the variance in the interpretation system, despite its highly distinct composition appearance.

In comparison, despite being positioned at the far-left end of the "composition spectrum" in Table 4, the Denmark glass F10 is still classified within Cluster 2, as depicted in Figure 4. If we only discuss UK glass, the trends observed in the evolution of flint container glass constituents will be the same, but in terms of specific numerical values, UK Cluster 2 exhibits an average MgO wt% of 1.81 wt% (1.787 wt% for all glasses), which is notably higher than the .716 wt% in UK Cluster 1 (1.238 wt% for all glasses, Indian glass has a great impact on this).

These data precisely demonstrate the variability in glass compositions related to geographical location, country, and even technological levels. In the following section, we will delve into this aspect further by combining it with other information using traditional analytical methods.

The direct inclusion of properties obtained from component calculations in the PCA analysis, along with the low-correlation components, would undeniably complicate data processing and impede the efficiency of common data organization strategies. Therefore, our approach gradually incorporates properties obtained from model calculations into the PCA clustering results. This enables us to observe the influence of components on glass properties.

In Figure 4A, the average melting temperature of Cluster 2, calculated from Fluegel[23] and Lakatos et al.[24] model, is higher than that of Cluster 1. Based on the previous analysis, if Cluster 2 represents the current composition of flint glass that differs from historical compositions, then the evolution of flint glass tends to favor higher melting temperatures.

A possible explanation for this is an improved understanding of how glass melts absorb radiative heat. Faber et al.[25] summarized the Rosseland mean absorption coefficients for flint, green, and amber glasses measured using

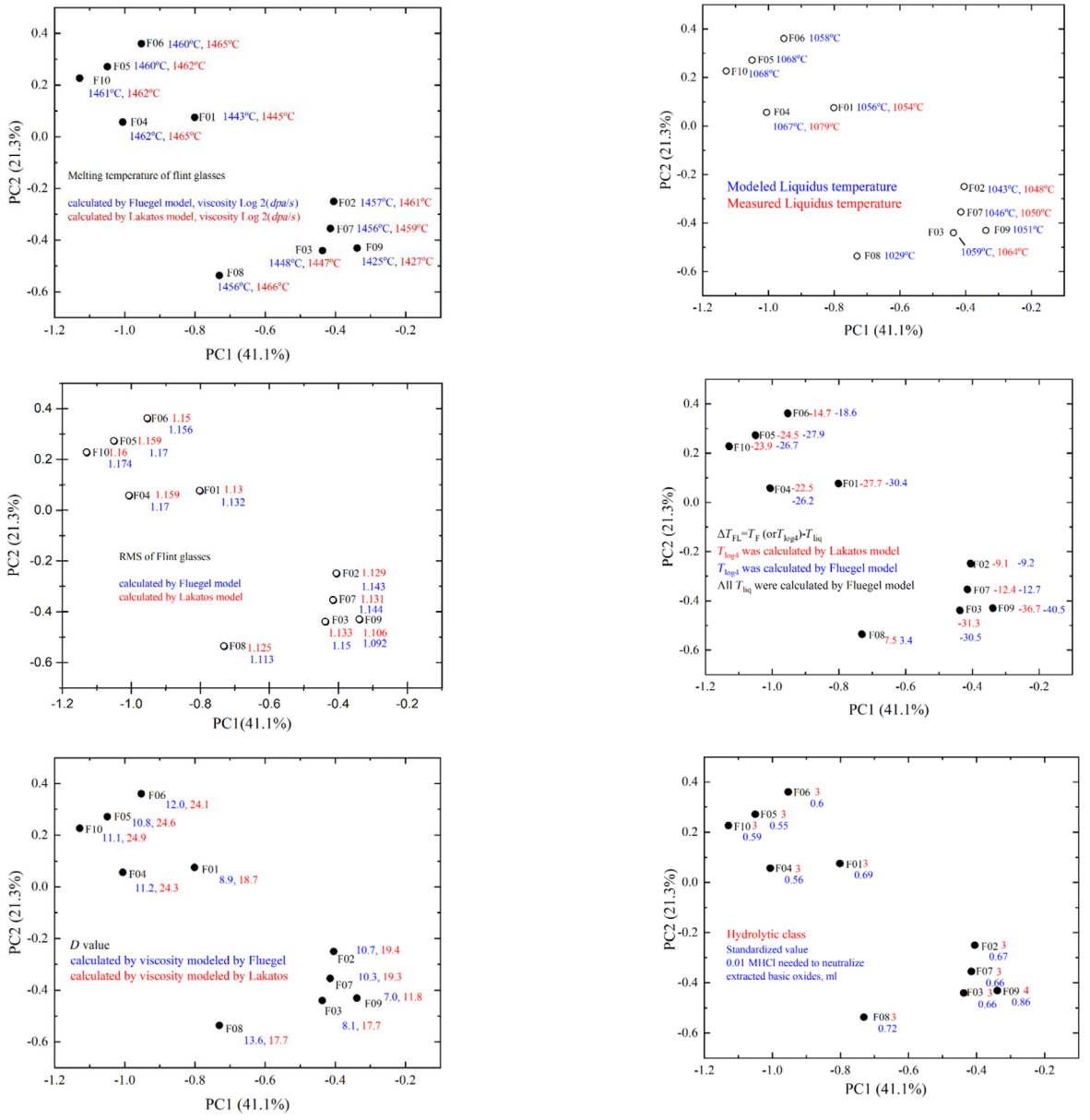

FIGURE 4 (A) Current flint container glasses melting temperatures distribution in principal component analysis (PCA) diagram. The viscosity log 2(*dpa*/*s*) values were calculated using the Fluegel[23] and Lakatos et al.[24] models separately and are listed in tab. 4A of Part 1. (B) Current flint container relative machine speed (RMS) distribution in PCA diagram. The viscosity values calculated using the Fluegel[23] and Lakatos et al.[24] models separately were used to estimate the RMS values, and these are listed in tab. 4A of Part 1. (C) Current flint container *D* value distribution in PCA diagram. The *D* values calculated using the Fluegel[23] and Lakatos et al.[24] models separately were used to estimate the RMS values, and these are listed in tab. 4A of Part 1. (D) Current flint container liquidus temperature distribution in PCA diagram. The modeled and measured liquidus temperatures were listed in tab. 4A of Part 1. (E) Current flint container ΔT_{FL} value distribution in PCA diagram. All ΔT_{FL} were listed in tab. 4A of Part 1. (F) Current flint container chemical durability value distribution in PCA diagram. Hydrolytic class and standardized values were listed in tab. 4A of Part 1.

FIGURE 4 Continued

the transmittance method developed by TNO, Eindhoven, in 1999 and the Orleans emissivity method in 2017, spanning temperatures from 500 to 1600°C. It was found that flint glass exhibits significantly lower absorption of thermal radiation compared to green and amber glasses. The longer mean free path of photons for radiative heat transfer in flint glass contributes to this lower absorption. Given that radiative heat transfer currently accounts for 70% of heat transfer in furnaces, flint glass melt in different regions to reach uniform high temperatures more rapidly, even though its melting point temperature is higher. In other words, the furnace temperature for melting flint glass could be appropriately lowered. However, upon recognizing this, manufacturers seem to have chosen not to reduce the furnace melting temperature of flint glass. Instead, they

have increased the batch melting temperature by adjusting the composition of flint glass. This decision serves two possible purposes: on one hand, it ensures that there are no significant fluctuations in the thermal regime of the same furnace due to color changes, and on the other hand, it provides more room for adjusting the glass composition to enhance glass quality and production rates.

Considering energy consumption, according to different statistical approaches, the average specific energy consumption for Soda-Lime-Silica glass furnaces in 2003 was around 5 GJ/t glass, which is about 25% of the average specific energy consumption in 1960.[17,26–28] In 2007, the average intensity of fuel consumption for the container glass industry in the European Union (EU) was 6.4 GJ/t of product.[29] According to the latest estimates,[30] the specific energy consumption of glass melting has remained approximately 3.24 GJ/t glass since around 2000. The reduction in energy consumption during the glass container melting process does not appear to be significant. This leads to an interesting question: since 2000, has the glass industry compensated for the increase in melting temperature with advancements in melting technology, and thus failed to make further progress in energy consumption as a singular indicator? This is a question worthy of future consideration.

In this context, the melting temperature of the Indian glass is particularly low, but its high alkali content not only results in higher raw material costs in certain regions but also undoubtedly shortens the lifespan of the melting furnace.[17,31] In this study, the Indian glass composition serves as a valuable reference point in comparison to the European and American regions. Due to the focus of this research on UK glass and limitations in space, further detailed discussion on F09 glass is not explored here, but will be elaborated in detail in Supporting Information A.

Among all other current flint container glasses, except for F09, the glass labeled as F01 and belonging to Cluster 2 exhibits the lowest melting temperature. In Figure 4B, the average relevant machine speed of Cluster 2, again, calculated based on the viscosity deduced from the Fluegel[23] and Lakatos et al.[24] model, is higher than that of Cluster 1. Special attention should still be given to the F01 glass that in Cluster 2, it has the lowest relative machine speed (RMS) in Cluster 2, but still high if compare it with Cluster 1. The trend of glass compositional evolution shows a preference for higher RMS. This point is easily understandable. As mentioned earlier, the relative increase in melting temperature certainly has its reasons. By effectively enhancing the production output per unit time, it can economically offset the slightly increased or unchanged fuel costs and may even prove to be more cost-effective. The corresponding practical evidence and technical details can be observed from the evolution of Individual Section (IS) machine performance speed. According to historical statistics,[32] the .3 L beverage bottling speed capability of IS machines has been on the rise since 1920, showing a linear increase from around 1950 to 2015. In the past 30 years, the speed for each cavity has increased from 420 containers produced per minute (cpm) in 1995–540 cpm in 2005, reaching 624 cpm in 2015.

In Figure 4C, the calculated D values of all glasses are all positive which indicate relative freedom from devitrification, particularly if the glass is fed to the forming machine at relatively low temperature or high viscosity.[17] Previously this D value was even higher, as reported by Zhernovaya et al.[33]: in 1977 values of D of container glasses were +29 (United States) and +39 (USSR). By 2010, a value of +15 was common in the global container glass industry[17] and all D values calculated by the Fluegel model are lower than +15, but the D values calculated by the Lakatos et al. model are between +15 and +29.

In Figure 4D, modeled liquidus temperatures are presented in PCA diagram. According to literatures,[17,11,34] a typical container glass liquidus temperature should be around 990–1050°C. However, except F02, F07 in Cluster 1 and F08, all other glasses are higher than 1050°C according to the Fluegel liquidus temperature model.[35] The liquidus temperatures of Cluster 2 are also higher than that of Cluster 1. The measured liquidus temperature is very close to the calculated temperature, and their trends align, providing further confirmation of the accuracy of the model calculations. The trend of continuously increasing liquidus temperature demonstrates the evolution of glass compositions with time and comprehensive technology.

ΔT_{FL}, the difference between forming temperature (T_F) and liquidus temperature (T_{liq}) is an important criterion that has been used successfully in the reformation of container glass and fiberglass compositions.[36,37] Negative ΔT_{FL} indicates an increased risk of devitrification during forming. Whether this would actually cause problems in reality is dependent largely on the particular conditions in a given furnace and forming operation. Some anecdotal evidence that some manufacturers operate with negative ΔT_{FL} quite safely.[17,36] In Figure 4E, the ΔT_{FL} of all glasses are negative, except for the F08 glass independent of Cluster 1 and Cluster 2, which is positive.

The criteria ΔT_{FL} and D provide useful methods for the estimation of the possibility of devitrification. In this study, most of the ΔT_{FL} values, except for the independent F12, fall within the high-risk region of devitrification. Bingham and Marshall's investigation around 2005[36] indicated that the ΔT_{FL} values of manufacturers at that time were close to zero, whereas in this study, the ΔT_{FL} values are significantly lower than zero. One possible explanation for this evolutionary trend is the advancement in

melting technology, which has led to increased production per unit area in the melting furnace. A case in point was that many manufacturers have already adopted the design of multiple electrode-assisted electric melting at the bottom of flame furnaces to enhance output. While the current emphasis on electric melting is for decarbonization purposes, its initial introduction was aimed at increasing the pull rate. The accelerated flow rate of the glass melt shortens its residence time in critical areas of the furnace, like the throat, resulting in a swift passage through this temperature zone during the cooling process. This significantly lowers the risk of crystallization and devitrification. The necessity to increase the production per unit area of the furnace has eased the devitrification requirements of compositions in this temperature range. It has been demonstrated that even if the liquidus temperature exceeds the working point, it does not cause issues. Furthermore, this change allows more flexibility in adjusting compositions to meet other performance requirements. It should be noted that the high liquidus temperature composition changes, along with the high RMS composition changes obtained from the model calculations mentioned earlier, are consistent with the production demands. One can be attributed to the need to increase the production per unit area of the furnace, while the other can be attributed to the need to increase the production per unit time.

The most convincing technical detail or key parameter for this is the daily output per unit area of the melting furnace, or specific pull rate. According to an internal factory report from 1911, the production capacity of European tank furnaces was approximately .36–.48 tons/day/m^2.[38] According to two different literatures, this sensitive parameter was around 1–3 and 2–3 around 1987 and 1991.[39,40] Based on an interview with an anonymous glass manufacturer, we learned that this figure increased from 3.15 and 3.4 to 3.9 and 3.7, respectively, between 2014 and 2024 in their plants. This indicates that furnace productivity has continuously improved through the efforts of people who works in glass industry, even in the past 20–30 years. Additionally, this objective data and detail strongly support our interpretation.

Discussions with a highly experienced industry veteran further confirmed this view, indicating that the melting rate of furnaces has been rising since 1999. Some furnaces have a maximum pull rate close to 4.0 tons/day/m^2 for flint glass, and around 3.5 tons/day/m^2 for amber or green glass. Clearly, not all furnaces always operate at their maximum melting rate. This depends on the job mix and the number of orders received or inventory requirements, but the trend is definitely upward. Additionally, two subjective intentions in furnace design and operation have been confirmed. First, since the first oil crisis in the 1970s, people have actively changed compositions to help molding achieve faster machine speeds, although they may not realize it, they have actually been doing this since the 1920s. Second, I would like to quote: "it's a bit of a holy grail to squeeze more out of the furnace and various boost configurations have been investigated but no breakthrough just yet." This represents a perennial challenge for furnace designers.

This progress can be attributed to recent advancements in furnace design methods, particularly the commercial application of computational fluid dynamics (CFD) technology, such as that provided by F.I.C. (UK) Limited in the United Kingdom and Glass Service in the Czech Republic. Additionally, there are significant related research within the academic community. For instance, studies by Beerkens,[41] Nìmec et al.[42] on the residence time of glass melt in the melting tank have enhanced our understanding of the melting process, dead water zones, and space utilization. These studies have greatly contributed to the optimization of furnace structures and increased productivity. Due to space limitations, further details are not discussed here.

For *D* value of current flint glasses, it related to the forming process (pertaining to the temperature difference between the annealing point and softening point) consistently remains in the positive range to prevent devitrification. Although it has slightly decreased compared to +15 in 2010 (calculated according to the Fluegel model), it still remains within a relatively safe region, as per the traditional perspective. This suggests that the development of forced cooling techniques during the forming process has progressed relatively slowly. A key bottleneck in the high-speed production of container glass is the rapid removal of heat from the glass during the molding process. For decades, advancements in mold cooling for automatic glass molding have primarily focused on designing air flow vertical channels and mold cooling shapes, such as plain and serrated fins, through CFD simulations.[43–45] However, all of these methods rely solely on air as the cooling medium. It is worth mentioning that the author has observed recent discussions in the industry about improving this situation. In future studies on compositional evolution, attention should be given to this parameter.

Figure 4F shows the variation of chemical stability in flint glass with respect to its composition, which is related to the glass quality. It can be observed that Cluster 2 requires a smaller volume average of HCl neutralization compared to Cluster 1, indicating that Cluster 2 exhibits stronger chemical stability. Additionally, we noticed that the three samples with the highest demand for HCl neutralization are F09 > F08 > F01, where F09 belongs to the fourth class of hydrolytic glass. Among these samples, F08

exhibits the poorest chemical stability after F09, followed by F01. However, all samples except F09 belong to the third class of hydrolytic glass.

Various standards, such as International Organization for Standardization (ISO) and British Standards (BS), have established permissible leaching limits for heavy metal oxides in glass containers, which are closely related to improvements in their chemical stability or water resistance. The progress in the chemical stability of glass products has been mandatorily enforced upon manufacturers under increasingly stringent and standardized requirements across various standards.

Over the past few decades, these standards, particularly ISO 7086/2, have evolved significantly to further reduce the leaching of lead and cadmium into food. The 1982 ISO 7086/2[46] allowed permissible limits for lead in large and small glass containers at 2.5 mg/L and 5.0 mg/L, respectively. The 2000 revision of ISO 7086/2[47] reduced these limits to .75 mg/L and 1.5 mg/L for large and small containers, respectively.

Since 1986, the BS 6748 standard[48] has set the maximum limits for lead and cadmium in Category 3 (packaging storage containers with a capacity greater than 3 liters) to below 1.5 mg/L and .1 mg/L, respectively. The 2011 revision[49] further standardized details such as analytical instruments and detection limits.

Some EU member states have defined separate requirements with limit values for glass food contact materials (FCM). For instance, France developed guidelines for inorganic materials to apply the EU FCM framework regulation 1935/2004.[50] The ISO-standard limits for lead (Pb) and cadmium (Cd) are applied. Additionally, they set a limit for chromium in fillable products at .03 mg/L. In the 2016 revision of the document,[50] the release limits for aluminum (Al), cobalt (Co), and arsenic (As) were also introduced.

Because the trend of the working range index (WRI) aligns with the D value, for simplicity, we will not delve deeper into the WRI at this stage. Since the variation in density is minimal and does not significantly contribute to the PCA analysis, the discussion on this aspect was omitted.

For individual samples, F01 should be a relatively optimized option. It is classified within the second cluster, exhibiting higher ΔT_{FL} and moderate RMS compared to other samples in this cluster. What sets it apart from the second cluster is its lowest melting temperature (except for F09). Additionally, its chemical stability is similar to other glasses (except for F09), falling into the third category. F08 does not belong to any of the clusters, with the lowest RMS (except for F09) and the unique positive ΔT_{FL}, suggesting there may be process control or equipment issues, resulting in its composition showing characteristics of reducing production risks and lower production speeds. F09, on the other hand, can be considered a significant representative of regional differences.

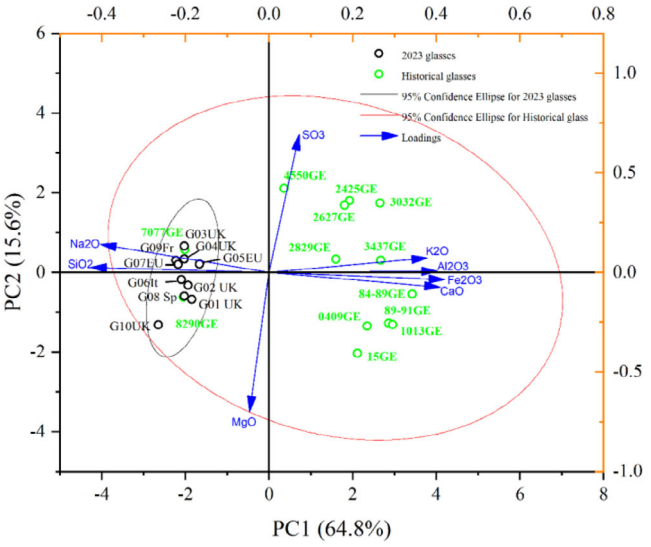

FIGURE 5 Principal component analysis (PCA; PC1 and PC2) of current Green container glasses composition (in black, Fr for France, It for Italy, and Sp for Spain) and historical German green glass composition from the record of Smrček[15] (in cyan, and marked according to the year and region, "GE" means Germany; "1013GE" means German glass from 1910 to 1913, for 19 century's glasses marked with "–," such as German glass from 1889 to 1891 was labeled as 89–91GE).

4.2 | Green container glasses

Figure 5 presents the PCA analysis results of the compositions of current green container glass and historical green glass composition data from Smrček's review,[15] for reference and comparison purposes. The record data from Germany are the most complete and thus chosen for this analysis.

The illustration reveals that the vast majority of historical German glass compositions are concentrated in the first and fourth quadrants. The glass compositions are arranged chronologically, following a counterclockwise direction from the fourth quadrant (1800–1913) to the first quadrant (1924–1950), then transitioning to the second quadrant (1970–1977), and finally returning to the fourth quadrant (1982–1990). The glass compositions from 1970 to 1977 and 1982–1990 show even distribution within the 95% confidence ellipse area of the current glass composition. This suggests that the modern green glass composition since 1970 closely resembles the current glass composition when historical glass compositions are used as a reference. Except for G10, which is slightly distant, the coordinates

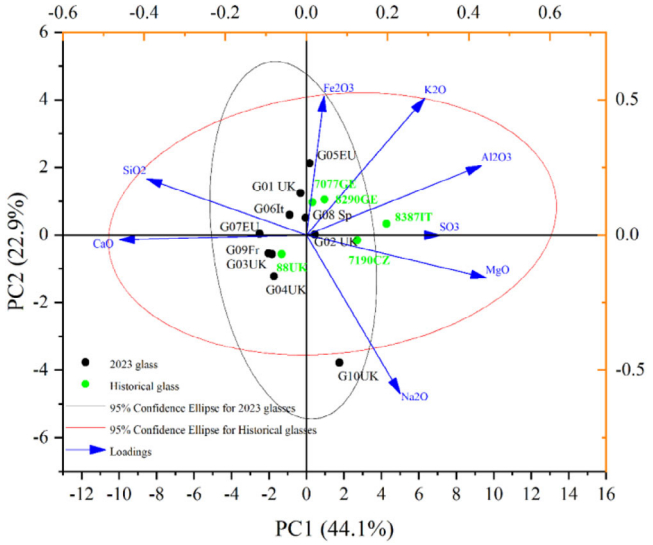

FIGURE 6 Principal component analysis (PCA; PC1 and PC2) of current green container glasses composition (in black, Fr for France, It for Italy, and Sp for Spain) and modern green glass composition from the record of Smrček[15] (in cyan, and marked according to the year and region, "GE" means Germany; "IT" means Italy; "CZ" means Czechia).

of the other current components are almost all situated between the historical compositions of 1970–1977 and 1982–1990.

Performing PCA analysis on the modern green glass compositions from various regions in Europe, together with the current green glass compositions (Figure 6), still poses challenges in separating them into distinct clusters. However, certain differences in the positions of these two types of glass can be observed. The modern European glass compositions primarily fall within the first quadrant, while the current glass compositions mainly occupy the second and third quadrants, except G10 falls within the fourth quadrant and far away from others. Considering the component loadings on the PCs, it is found that in the primary direction of PC1 (44.1%), the current glass exhibits higher CaO and SiO_2 content compared to modern European glass. Conversely, current glasses (except G10) show relatively higher levels of SO_3, MgO, and Al_2O_3.

In contrast to the cautious analysis conducted previously on flint glass, we directly perform a PCA analysis on the high temperature properties (which are not entirely unrelated) of the current green glasses based on different models and are according to each other (Figure 7A,B). This analytical approach is noticeably more concise. It is worth noting that if we consider the different origins of the samples, a clear boundary can be drawn between the samples from the United Kingdom and those from other countries. In other word, non-UK or European continental glasses.

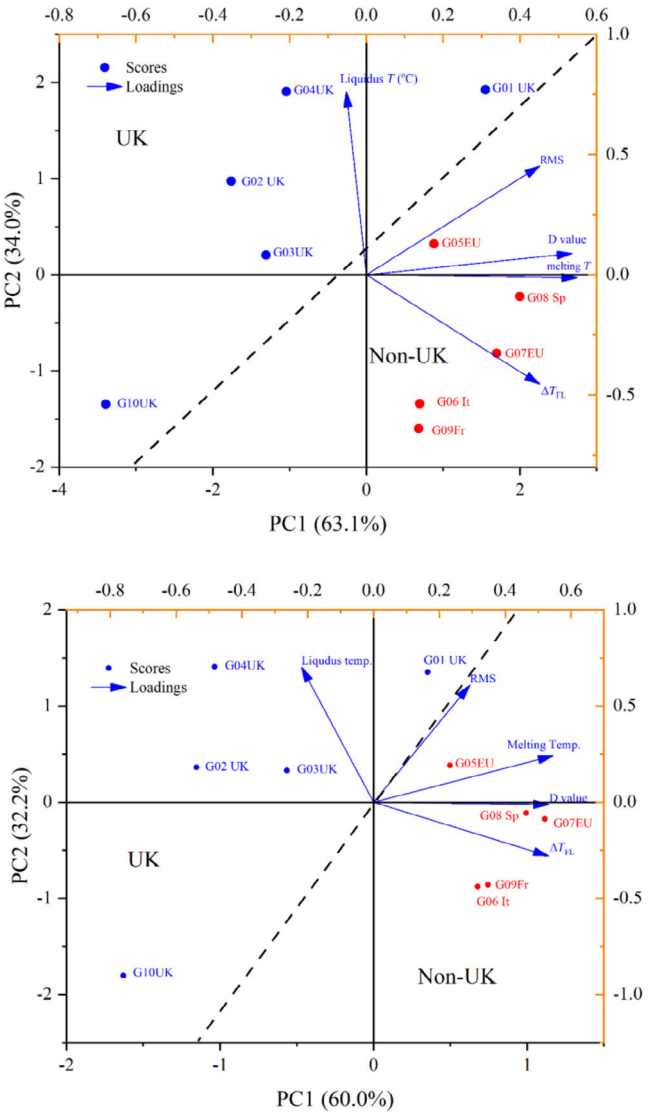

FIGURE 7 (A) Principal component analysis (PCA; PC1 and PC2) of high temperature properties of current green container glasses (all properties values were listed in tab. 4A of Part 1). (B) PCA (PC1 and PC2) of high temperature properties of current green container glasses (all properties values were listed in tab. 4A of Part 1).

The illustration shows that both the Fluegel[23] and Lakatos et al.[24] models have rightward loadings of the main property variables related to viscosity, primarily contributing to PC1. This suggests that higher melting temperatures correspond to higher RMS, *D* value, and ΔT_{FL} values. However, the contribution of the liquidus temperature loading to PC differs from that of other property variables.

According to the Fluegel model, the G10 sample, which was in the third quadrant, exhibits a particularly low value in the loading direction of the melting temperature, and its RMS is also the lowest (1.084, with a mean of 1.129). From an optimization perspective, the G04, G02, and G03 samples located in the second quadrant are relatively

reasonable compared to the other components in the first and fourth quadrants. They have lower melting temperatures, and their RMS values are roughly comparable to those of the samples in the first and fourth quadrants. Notably, the G04 sample has the highest RMS, and its melting temperature is about 15–20°C lower than that of the samples in the first and fourth quadrants.

From a process control perspective, all glass samples exhibit positive D values, and all ΔT_{FL} values are negative, which aligns with the previously mentioned flint glass. Considering only ΔT_{FL} and since all D values fall within the positive range, the glass samples in the first and fourth quadrants have the lowest process control difficulty, while those in the second quadrant face the highest difficulty. The G10 sample falls in the middle of the glass samples in the second quadrant. Additionally, among all the glass samples, G04 has the lowest ΔT_{FL}, implying that optimizing the melting temperature and RMS simultaneously places higher demands on the glass melting and forming process control.

The PCA analysis results based on the Lakatos et al. model are similar to those of the Fluegel model, with only slight data position shifts, but they do not have any significant impact on the final result analysis. Therefore, no further elaboration is necessary.

Although the composition of the current green glasses is not significantly different from historical compositions, we are still interested in understanding the correspondence between their composition and properties. To eliminate the interference of other components on the sample composition scores (Figures 5 and 6), a separate PCA analysis was performed on the current glass compositions as variables, as shown in Figure 8. From Figure 8, a clear boundary can be drawn between the samples from the United Kingdom and those from other countries.

Along the Na_2O loading direction, the samples from the United Kingdom, namely, G10, G04, G02, and G03, have relatively higher values compared to samples from other regions (with Na_2O content above 13 wt%, differing from other glass compositions by approximately .5%–1%). Since the sample scores/positions are influenced by the comprehensive effect of each loading, the order of sample scores along the variable loading direction is not strictly arranged according to the content of a particular variable, such as Na_2O. This observation suggests that the reduction of glass melting points is significantly related to Na_2O content.

Meanwhile, in the direction of SiO_2 loading, G04, G02, and G03 are located close to the majority of other glass samples. In terms of CaO loading, G04 has the highest position (and indeed the highest CaO wt%), which explains why it has the highest RMS value. This further indicates that high-yield, low-melting-point compositions not only require strict production process requirements but may also have relatively higher overall raw material costs due to the relatively expensive price of soda ash.

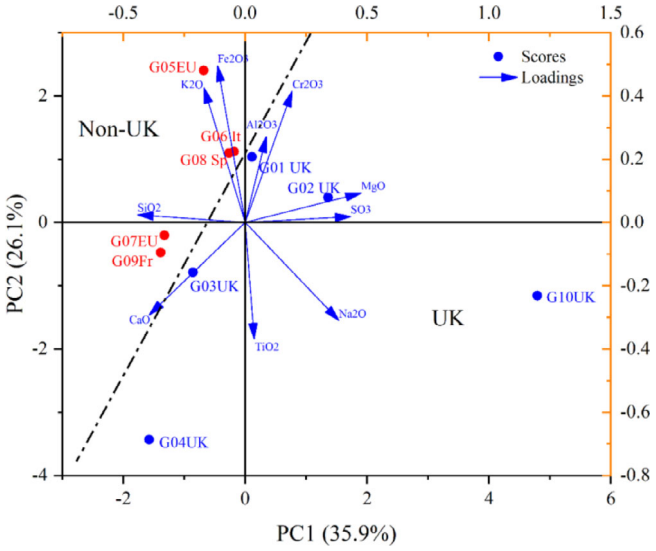

FIGURE 8 Principal component analysis (PCA; PC1 and PC2) biplot of current green container glass composition.

Among this group of green glasses, G10 exhibits some issues that warrant analysis, It occupies an unfavorable position in both performance and composition PCA plots (high alkali content, low RMS). Interestingly, when comparing the best and worst performing glasses, G10 and G04, both belong to British glass compositions. The reasons for this phenomenon are consistent with the previous analysis of flint glass. Analyzing based solely on composition is one-sided; it requires a comprehensive analysis in conjunction with the conditions of the production process and equipment.

To encapsulate, when compared separately with historical glass compositions and modern glass compositions since the 1970s, the green glass compositions do not exhibit significant differences. However, we should note that the proportion of UK glass to other regional glasses in the green glass dataset is 5:5, while in the Flint glass dataset, this proportion is 8:2. Due to the challenges in obtaining a sufficient number of British glass samples during the sample collection process, this regional diversity could potentially weaken the significance of the relative changes in current compositions compared to historical compositions.

Nevertheless, based on the analysis of composition–property relationships, two distinct levels of compositions are observed in the current glass compositions, and they are indeed somewhat related to regional variations (UK and European continental glasses).

Represented by G04, G02, and G03, the UK glasses have relatively lower melting points due to higher Na_2O while

maintaining similar RMS values. Among them, G04 stands out as an optimized representative composition.

4.3 | Amber container glasses

Figure 9A presents the PCA analysis results of the compositions of current amber container glass and historical amber glass composition data from Smrček's review.[15] In comparison to flint and green glass, historical composition records for amber glass are notably incomplete, encompassing only five recorded data points for the most prolific German glass since 1913. Records from other countries are even more scarce. Hence, we included two historical data points from the United Kingdom in the PCA analysis to enhance comprehensiveness.

It is evident that although the glass composition scores/positions of 2023 fall within the 95% confidence ellipse region of historical glass, their data distribution differs noticeably from that of historical glass. Furthermore, the evolutionary direction of historical glass composition scores is precisely opposite to the direction of the sodium oxide loading vector, pointing toward the region of historical glass compositions. The three modern glass compositions since 1972 unfold along the periphery of the current glass composition and do not overlap with it. Compared to the region of historical glass composition scores, the region of current glass compositions is characterized by low sodium oxide, high iron oxide, high calcium oxide, and high sulfur. The content variations of silicon dioxide, aluminum oxide, and magnesium oxide are not significant.

To compare modern European amber glass compositions since the 1970s with the current glass compositions, a considerable quantity of modern European amber glass compositions were incorporated into Figure 9B and underwent PCA analysis together with the glass compositions from the present study. Notably, there is an observed overlap in the 95% confidence ellipse regions of the two, particularly evident with A04 and A05, which are relatively near the range of modern glass compositions. Nevertheless, the distinctions in the composition scores/positions between other current glass compositions and modern glass are also distinctly apparent. The current glass compositions are predominantly situated in the first and fourth quadrants, whereas modern glass compositions exclusively reside in the second and third quadrants. Only A10, A04, and A05 are positioned within the second quadrant. Looking at the contribution directions of composition variable loadings, except for A04, A10, and A05, the current glass has relatively higher levels of aluminum and potassium compared to modern glass compositions since the 1970s, while the content of silicon dioxide is relatively lower. The calcium oxide content of all current glass com-

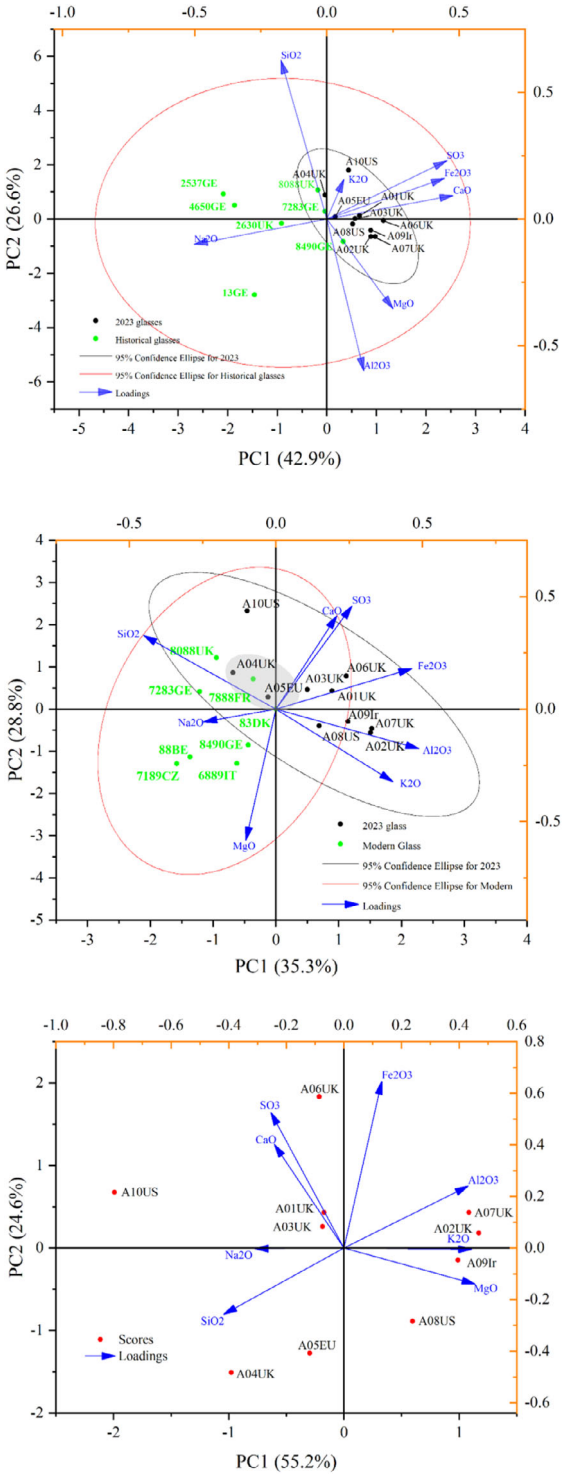

FIGURE 9 (A) Principal component analysis (PCA; PC1 and PC2) of current amber container glasses composition (in black, Ir for Ireland) and historical amber glass composition from the record of Smrček[15] (in cyan, and marked according to the year and region, "GE" means Germany). (B) PCA (PC1 and PC2) of current amber container glasses composition (in black, IE for Ireland) and modern amber glass composition (since 1970s) from the record of Smrček[15] (in cyan, and marked according to the year and region, "GE" means Germany, "IT" means Italy, "BE" means Belgium, "CZ" means Czechia, "DK" means Denmark, and "FR" means France). (C) PCA (PC1 and PC2) of current amber container glasses composition.

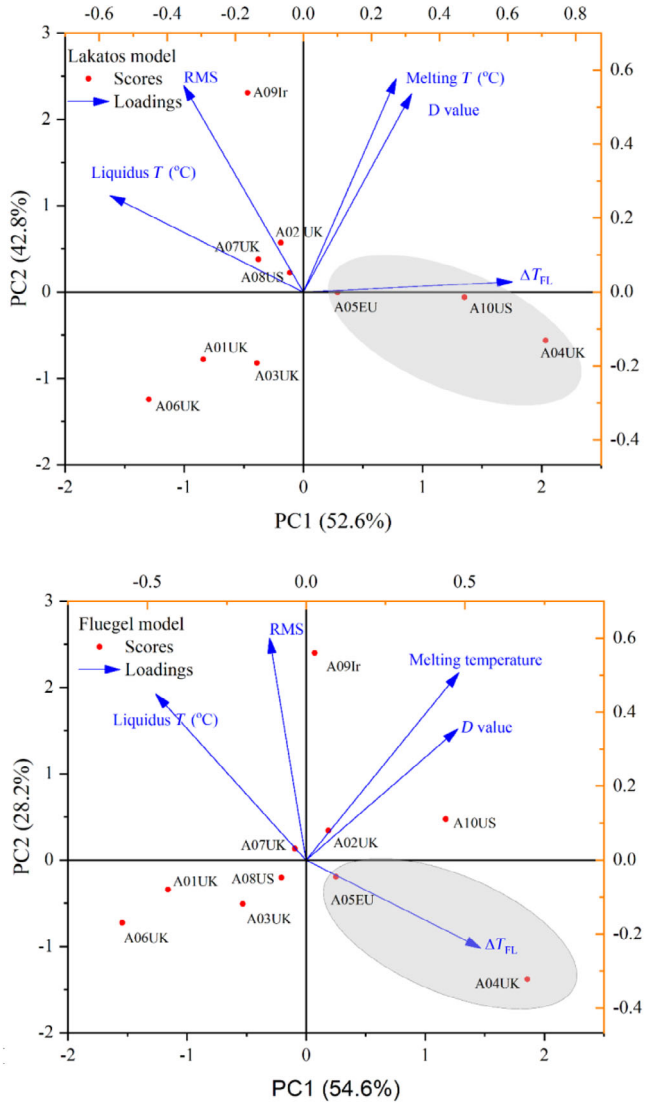

FIGURE 10 (A) Principal component analysis (PCA; PC1 and PC2) of high temperature properties of current amber container glasses (all properties values were listed in tab. 4A of Part 1). (B) PCA (PC1 and PC2) of high temperature properties of current amber container glasses (all property values were listed in tab. 4A of Part 1). RMS, relative machine speed.

positions is higher compared to modern glass. This PCA plot reflects the changes in amber glass compositions over the past 50 years.

To understand the correspondence between current compositions and properties, and to eliminate the interference of historical compositions on sample composition scores, as shown in Figure 9C, we conducted a separate PCA analysis on the current glass compositions as variables. Figure 10 illustrates the PCA of the calculated high-temperature performance results of current amber glass based on the Fluegel[23] and Lakatos et al.[24] viscosity models. From the figure, it can be observed that the loadings of various high-temperature performance components calculated based on different viscosity models, as well as the positions of the sample scores, are generally similar. Therefore, here we consider the statistically oriented Fluegel model Figure 10A as the reference and discuss its results in conjunction with the PCA results of the current compositions.

Taking the information above into consideration, these 10 samples can be grouped into three main categories in Figure 10A. A04, A05, and A10 constitute the first group (in gray area as show in diagram); A01, A03, and A06 form the second group; while A07, A02, A08 and A09 make up the third group.

As shown in Figure 9B, the first group of compositions closest to the region of modern glass compositions forms a cluster in the PCA analysis of high-temperature performance in Figure 10A,B, situated in the fourth quadrant and marked with the gray region. According to the composition analysis in Figure 9C, the first group glasses are high in SiO_2 and Na_2O. According to the properties analysis in Figure 10A,B, the ΔT_{FL} of group one glasses is higher than others, D value is high, melting temperature is around 1450°C, but RMS is relevant low. This indicates that the production process difficulty for the first group of glasses, which is similar to modern glass, is low. The melting temperature is normal, but due to higher sodium oxide content, its raw material costs might be higher. Additionally, it may not demand a relevant high production rate within a unit of time.

For the second group glasses, as shown in Figure 9C, the positions of the second group of glass compositions are located in the second quadrant and closely aligned with PC1 = 0 axis. The second group features higher contents of calcium dioxide, iron, and SO_3. In terms of performance, as we can see from Figure 10, the second group has the lowest melting point. In Figure 10B, if a line is drawn from A06 toward A10, this line is nearly perpendicular to the RMS vector. This implies that the RMS of the second group of glasses (A01, A03, and A06) is at an average level (almost same as A08, A07, A02, A05, and A10). However, relatively speaking, its ΔT_{FL} and D value indicators are comparatively lower.

The analysis above indicates that the second group of glass has the lowest melting cost and carbon emissions associated with the melting process. Due to the lower sodium oxide content, the raw material costs are relatively lower compared to the first group of glass (compositions resembling glasses from the 1970s to 1990s). Additionally, its composition can meet the requirements for high-speed production. However, its production process demands are stringent, requiring advanced production equipment and high-level control. It represents a relatively advanced direction for compositional development.

The third group of glass, as shown in Figure 9C, has compositions located in the first and fourth quadrants of the composition PCA analysis. Its composition is characterized by low SiO_2 and Na_2O content, high Al_2O_3, K_2O, and MgO content. Among them, the composition of A08 is relatively distant in terms of score/position compared to other glass compositions in the third group. In terms of thermal properties, A02, A07, and A08's melting temperatures are higher than group 2 but lower than group 1. RMS is comparable to that of the second group. D value and ΔT_{FL} also falls between groups 1 and 2. Except A09, which has the highest melting temperature and RMS, low ΔT_{FL} and high D value. The analysis seems to indicate that the overall assessment of the third group's properties, except for A09, falls between the first and second groups (for composition, in Figure 9A, the third group [A07, A08, A02, and A09, situated in the fourth quadrant] is relatively further away from the first group [A01, A03, A06, situated in the first quadrant] compared to the second group [A04, A05, A10, situated in the second quadrant]). Its production process difficulty is moderate, melting energy consumption is intermediate, and production speed is similar to the second group. However, in terms of raw material selection, it adopts a composition with less alkali and a higher feldspar content, resulting in relatively lower raw material costs. However, it is important to emphasize that the patterns in other properties of current amber glass are different. Specifically, the density of the first group of glasses is lower than that of the second group, and all glasses fall into hydrolytic class three.

In summation, the current amber glass compositions show significant differences compared to those from the 1970s to the 1990s. The evolution of these compositions has two main directions: one focuses on reducing the raw material costs of glass by using a combination of low soda and high feldspar materials, while the other aims to lower the melting point by high proportion of CaO (A06 and A01). Both directions exhibit characteristics of relatively high RMS and low ΔT_{FL}. This indicates that current amber glass, similar to flint glass, is evolving toward higher production rates and greater output capacity.

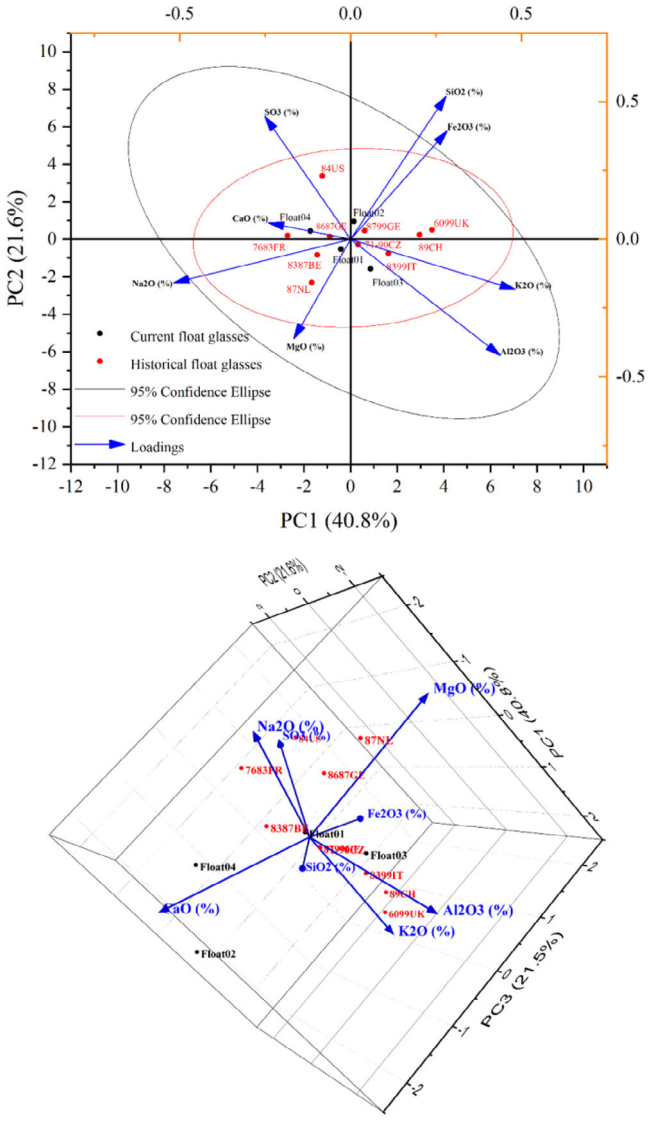

FIGURE 11 (A) Principal component analysis (PCA; PC1 and PC2) of current float glasses composition (in black) and historical float glass composition (in red) from the record of Smrček[14] (in red, and marked according to the year and region, "GE" for Germany; "CZ" for Czechia; "CH" for Sweden; "IT" for Italy; "BE" for Belgium; "FR" for France; "NL" for the Netherlands; and "US" for United States). (B) PCA (PC1, PC2 and PC3) of current float glasses composition (in black) and historical flint glass composition (in red) from the record of Smrček.[14]

4.4 | Float glasses

Collecting float glass samples was not as easy as container glass samples. Fortunately, in an unfortunate situation, four manufacturers were willing to anonymously provide their float glass samples from 2022 to 2023. Due to the limited number of samples and the shorter history of float glass development (invented by Pilkington in the 1950s in St Helens[32]) compared to container glass, as well as the more complex production processes and slightly different performance parameters considered, we could not conduct an in-depth study like we did with container glass. The performance data resulting from the composition testing and calculations have been listed in the above tables for reference and future research. The data are self-explanatory, and there is no need to elaborate further here. However, we can still compare their compositions with historical records for a glimpse into the patterns within it.

Figure 11A presents the PCA analysis results of the compositions of float glasses. Historical glass composition float

of glasses from Smrček's review[14] is included in the diagram for reference and comparison purposes. It is evident that in the PC1 and PC2 biplots, the 95% confidence ellipse regions of current and historical glass compositions largely overlap, which explain 62.4% of the variance in the system. This indicates that within this range, current glass compositions do not appear to be very similar to historical compositions. For further exploration, the composition PCA was extended to PC3 as shown in Figure 11B, which PC3 accounts for 21.5% of the variance and collectively explain 83.9% of the variance in the interpretation system. In the direction of PC3, Float 02 and Float 04 are distant from Float01, 03, and other historical glass compositions. Additionally, the CaO loading has the most prominent contribution to PC3, indicating that the high calcium oxide content in Float 02 and Float 04 sets them apart from other current and historical glass compositions.

5 | CONCLUSIONS

Research on the historical data of commercial glass indicates that the 1970s mark a significant turning point in the composition of all different color container glasses. Research on flint (colorless) container glass compositions obtained from the UK market in 2022–2023 suggests that current compositions are undergoing a transitional phase compared to from the period from the 1970s to the 1990s. Meanwhile, regional differences in glass compositions are also quite evident. Through the analysis of glass compositions and properties, we have identified that the main reasons for this shift in composition trends include: "More," referring to higher production output per unit area within a given time frame, which can be observed through the relaxation of requirements regarding the ΔT_{FL}; "Faster" denoting accelerated forming processes due to higher RMS; and "Better" indicating enhanced chemical durability. It is shown that glass production is influenced by multiple factors, not just compositional design. The coordination of other production processes also serves the purpose of improving economic optimization. Current flint container glass composition designs take into account, but are not limited to, the reduction in raw material costs (e.g., low soda). Meanwhile, the trend in current glass composition development indicates prioritizing meeting the demands of high-speed production and low cost of batch materials over reduced furnace temperatures. For individual samples, F01 appears to be the most optimized option with the lowest melting temperature among the surveyed European glasses. It exhibits good chemical durability, moderate RMS, as depicted in the PCA diagram of flint glass compositions, where it falls within the second cluster representing the evolutionary direction.

For green container glass, most current compositions do not exhibit significant differences from compositions since the 1970s. Based on the analysis of composition–property relationships, two distinct levels of composition were observed in the current glass compositions, and they are indeed somewhat related to regional variations (UK and European glasses).

Current amber container glass compositions show significant differences compared to those from the 1970s to the 1990s. The evolution of these compositions has two main directions: one focuses on reducing the raw material costs by using a combination of low soda and high feldspar materials, while the other aims to reduce the melting temperature by using a higher proportion of CaO. Both directions exhibit characteristics of relatively high RMS and low ΔT_{FL}. This indicates that current amber container glass, similar to flint container glass, is evolving toward higher production rates and greater output capacity. From the perspective of reducing CO_2 emissions, glasses A06 and A01 are recommended here due to their higher CaO contents, which not only lower the melting temperature but also enhance production efficiency.

Current float glass compositions do not show significant differences compared to historical recorded compositions, however, this may be due to the limited number of samples available to this study (only four). Under these limited conditions, the compositions of 2 of the samples exhibited a notably higher CaO content compared to other current glass compositions and historical recorded compositions. This may suggest a move to decrease melting temperatures, however, further research to include a larger sample set is suggested.

ACKNOWLEDGMENTS

Wei Deng and Paul A. Bingham express gratitude for the financial support received from UKRI/EPSRC (TransFIRe Hub, EP/V054627/1). The authors also extend their appreciation to Dr. Nick Kirk and Mr. Adam Frith from Glass Technology Services Ltd., Stuart Hakes from F.I.C. (UK) and anonymous glass manufacturers for valuable discussions and technical assistance. For the purpose of open access, the authors have applied a Creative Commons Attribution (CC BY) license to any Author Accepted Manuscript version arising from this submission.

REFERENCES

1. Keppeler G. Untersuchungen an Flaschengläsern. Glastech Ber. 1930;8:65–77.
2. Keppeler G. The composition and properties of the chief types of commercial glasses. J Soc Glass Technol. 1937;21:415–27.
3. Keppeler G, Maenicke R. Zur Kenntnis der Flaschengläsern mit besonderer Berücksichtigung ihrer Haltbarkeit. *Sprechsaal*. 1951;64:7–10, 28–30, 65–68.

4. Keppeler G, Goetzke H. Untersuchungen an Flaschengläsern der Nachkriegszeit. Glas-Email-Keram-Techn. 1931;2:134–38.
5. Moore H, Lyle AK. Container glass compositions 1932–1946. Glass Ind. 1947;28:563–66.
6. Allen AG, Lyle AK. Container glass compositions-1947. Glass Ind. 1948;29:493–594.
7. Loesell RE, Lester WR. Container glass compositions 1932 to 1960. Glass Ind. 1961;42:623–62.
8. Lyle AK. Design and development of glasses for manufacture of containers. Glass Ind. 1961;42:252.
9. Stadler L, Cronin D. Container glass composition. Glass Ind. 1977;58:10–33.
10. Stadler L, Cronin D. Part 2 container glass composition. Glass Ind. 1978;59:10–13.
11. Turbulent times 1980-1989 [cited 2023 Dec 31]. Available from: https://emhartglass.com/history
12. Katkova KS, Balandina TI, Krylova GN, Belyaeva AG, Guseva NB. Analysis of industrial packaging glass compositions and basic trends in their optimization. Glass Ceram. 1985;42:257–59.
13. Smrček A. European container glasses 1982 to 1988. Glastech Ber. 1990;63:309–17.
14. Smrček A. Evolution of the compositions of commercial glasses 1830 to 1990. Part 1. Flat glass. Glass Sci Technol. 2005;78:173–84.
15. Smrček A. Evolution of the compositions of commercial glasses 1830 to 1990. Part II. Container glass. Glass Sci Technol. 2005;78:230–44.
16. Smrček A. Evolution of the compositions of commercial glasses 1830 to 1990. Part III. Pressed glass. Glass Sci Technol. 2005;78:287–94.
17. Wallenberger FT, Bingham PA. Fiberglass and glass technology: energy-friendly compositions and applications. New York: Springer; 2009.
18. Tong K. Analysis of glass relics based on principal component analysis and k-means clustering. J Phys Conf Ser. 2023;2608:012017.
19. Zheng T, Gong Z, Chen Y, Ma Q. Composition analysis of ancient glass products based on logistic regression and principal component analysis. Adv Comp Signals Syst. 2023;7:92–101.
20. Baxter MJ, Beardah CC, Cool HEM, Jackson CM. Compositional data analysis of some alkaline glasses. Math Geol. 2005;37:183–96.
21. Jolliffe IT, editor. Principal component analysis for special types of data. In: Principal component analysis. New York, NY: Springer; 2002. p. 338–72.
22. Gaines LL, Mintz MM. Energy implications of glass-container recycling. Argonne, IL, United States: Argonne National Lab. (ANL); Golden, CO, United States: National Renewable Energy Lab. (NREL); 1994.
23. Fluegel A. Glass viscosity calculation based on a global statistical modeling approach. Glass Technol-Part A. 2007;48:13–30.
24. Lakatos T, Johansson LG, Simmingskold B. Viscosity temperature relations in the glass system SiO_2-Al_2O_3-Na_2O-K_2O-CaO-MgO in the composition range of technical glasses. Glass Technol. 1972;13:88–95.
25. Faber AJ, Rongen M, Lankhorst A, Meneses DDS. Characterization of high temperature optical spectra of glass melts and modeling of thermal radiation conductivity. Int J Appl Glass Sci. 2020;11:442–62.
26. Good Practice Guide 127. Energy efficient environmental control in the glass industry. London, UK: The Carbon Trust; 2000.
27. Energy Consumption Guide ECG027. Energy use in the container glass industry. London, UK: The Carbon Trust; 2005.
28. G.M.I. Council, Ross CP, Tincher GL. Glass melting technology – a technical and economic assessment. Westerville, OH: Glass Manufacturing Industry Council; 2004.
29. Schmitz A, Kamiński J, Maria Scalet B, Soria A. Energy consumption and CO_2 emissions of the European glass industry. Energy Policy. 2011;39:142–55.
30. Kahl SR. Sustainable container glass making until 2030 and beyond. Furnace solutions 2023. Saint Helens, UK; 2023.
31. Allendorf MD, Spear KE. Thermodynamic analysis of silica refractory corrosion in glass-melting furnaces. J Electrochem Soc. 2001;148:B59.
32. Richet P, editor. Encyclopedia of glass science, technology, history, and culture. Vol. I. New Jersey: Wiley; 2021.
33. Zhernovaya NF, Onishchuk VI, Kurnikov VA, Zhernovoi FE. Rapid evaluation of the workability of container glass. Glass Ceram. 2001;58:329–31.
34. Hrma P, Smith DE, Matyáš J, Yeager JD, Jones JV, Boulos EN. Effect of float glass composition on liquidus temperature and devitrification behaviour. Glass Technol. 2006;47:78–90.
35. Fluegel A. Modeling of glass liquidus temperatures using disconnected peak functions. In: Glass and optical materials division meeting, Rochester, NY, USA; 2007.
36. Bingham P, Marshall M. Reformulation of container glasses for environmental benefit through lower melting temperatures. Glass Technol. 2005;46:11–19.
37. Wallenberger FT, Hicks RJ. The effect of boron on the properties of fibreglass melts. Glass Technol. 2006;47:148–52.
38. Richet P, editor. Encyclopedia of glass science, technology, history, and culture. Vol. II. New Jersey: Wiley; 2021.
39. Woolley FE. Melting/fining. In: Schneider SJ, Vol Chairman. Engineered materials handbook. Vol. 4. Ceramics and glasses. USA: ASM International; 1991. p. 386–93.
40. Trier W. Glass furnaces design construction and operation [English]. Loewenstein KL, translator. Sheffield: Society of Glass Technology; 1987.
41. Beerkens R. Analysis of elementary process steps in industrial glass melting tanks: some ideas on innovations in industrial glass melting. Ceramics-Silikaty. 2008;52:206–17.
42. Nìmec L, Jebavá M, Cincibusová P. The removal of bubbles from glass melts in horizontal or vertical channels with different glass flow patterns. Ceramics-Silikaty. 2006;50:140–52.
43. Rosa N, Costa J, Lopes AG. CFD study of transient heating and cooling of a blank mould with a conformal cooling channel for manufacturing glass containers. Results Eng. 2023;17:100932.
44. Ngankeu PS. Improvements to Emhart glass vertiflow mold cooling applications in glass container production. In: 76th conference on glass problems. 2016. p. 185–91.
45. Sereno P, Frade J. Improvement of mold cooling for automatic glass molding—a preliminary geometry study on representative test specimens. Mater Proc. 2022;8:92.
46. ISO 7068 -2. Glassware and glass ceramic ware in contact with food—release of lead and cadmium—Part 2: permissible limits. First edition - 1982-11-15.

47. ISO 7068 -2. Glass hollowware in contact with food—release of lead and cadmium—-Part 2: permissible limits. Second edition 2000-03-01.
48. BS 6748:1986. Specification for limits of metal release from ceramic ware, glassware, glass ceramic ware and vitreous enamel ware.
49. BS 6748:1986+A1:2011. Specification for limits of metal release from ceramic ware, glassware, glass ceramic ware and vitreous enamel ware.
50. Direction Générale de la Concurrence, de la Consommation et de la Répression des Fraudes. Matériaux inorganiques (hors métaux et alliages) [cited 2024 July 31]. Available from: https://www.economie.gouv.fr/dgccrf/materiaux-inorganiques-hors-metaux-et-alliages

SUPPORTING INFORMATION

Additional supporting information can be found online in the Supporting Information section at the end of this article.

How to cite this article: Deng W, Wakelin E, Kilinc E, Bingham PA. A survey of commercial soda–lime–silica glass compositions: Trends and opportunities II—Principal component analysis (PCA) of glass compositions. Int J Appl Glass Sci. 2024;1–18. https://doi.org/10.1111/ijag.16689